Am J Transl Res 2018;10(7):2087-2101
www.ajtr.org /ISSN:1943-8141/AJTR0077075

Original Article

The change of synovial fluid proteome in rabbit surgery-induced model of knee osteoarthritis

Qinglu Luo[1,2], Xi Qin[1], Yaxian Qiu[1], Lingying Hou[1], Ning Yang[1]

[1]The Fifth Affiliated Hospital of Guangzhou Medicine University, Guangzhou 510700, Guangdong, China; [2]School of Rehabilitation, Fujian University of Traditional Chinese Medicine, Fujian 350122, China

Received March 30, 2018; Accepted June 9, 2018; Epub July 15, 2018; Published July 30, 2018

Abstract: The aims of this study were to explore the change of synovial fluid (SF) proteome in a knee osteoarthritis (KOA) rabbit model, and to provide a new target for the treatment of knee osteoarthritis at the proteomic level. Sixteen New Zealand rabbits were randomly and equally divided into two groups. Group A rabbits were subjected to right anterior cruciate ligament transection (ACLT), while group B rabbits were subjected to sham ACLT. Six weeks later, the proteomes of knee joint SF from group A and B rabbits were analyzed using a label-free quantitative proteomic analysis method. We extracted 944 relevant items from GO BlastGO2 for the 23 proteins differentially expressed between the two groups. The final annotation results were 23 protein sequences annotated by 462 GO items. According to the KEGG gene database of rabbit protein sequences, as well as annotation of the KO numbers of homologous/similar proteins to the relevant 64 KEGG pathways, we extracted the sequences of 16 significantly differently expressed proteins among the relevant 64 KEGG messages/metabolism pathways. These included adiponectin, pyruvate kinase, bisphosphoglycerate mutase, HtpG/heat shock proteins, hemoglobin subunit alpha-1 2, VCP (CDC48), 14-3-3 protein beta/theta/zeta, and ferritin heavy chain, whose levels were decreased in group A. The other proteins were fibrinogen alpha/beta/gamma chain, carboxylesterase 2, paraoxonase/arylesterase 1, apolipoprotein A-I, immunoglobulin heavy chain, and transferrin, whose levels were increased in group B. The identified differentially expressed proteins indicate the change of SF proteomic expression in KOA and may provide protein targets for treating this condition.

Keywords: Proteome, synovial membrane, osteoarthritis, synovial fluid

Introduction

Osteoarthritis (OA) is a common cause of musculoskeletal disability. The main pathological change of OA is progressive articular cartilage degeneration, however, synovitis is another major factor in the development of OA [1, 2]. Some researchers regard synovitis as the main cause of pain and edema in OA patients [3]. In OA the synovial volume increases because the synovial membrane becomes inflamed and secrets synovial fluid (SF) and its components, such as tumor necrosis factor (TNF) and interleukins (ILs) [4]. Decreasing the degree of synovitis is an important aim in OA therapy.

Some of the proteins in SF are secreted by the synovial membrane or chondrocytes or result from a diffusion process from abnormally elevated plasma levels. Therefore most studies have assayed blood markers as indicators of SF inflammation. But some inflammation markers of SF cannot diffuse into blood; therefore, direct investigation of SF should confirm the pathological change of OA.

Recently, reports have been published on studies of human or animal articular synovial fluid (SF) and cartilage proteomes using isobaric tags for relative and absolute quantification (iTRAQ) or mass spectrometry (MS) [5-7]. However, changes in synovial fluid proteins of a rabbit model of knee osteoarthritis (KOA) have not been reported, so in this study we aimed to determine the change of synovial fluid proteome in a surgery-induced rabbit model of knee osteoarthritis (KOA).

Materials and methods

Animals

Sixteen healthy 6-month-old New Zealand white (NZW) rabbits (eight male, eight female), wei-

ghing 2.5~3.0 kg, were recruited. All protocols were in line with national legislation and guidelines for laboratory animal care and use of the People's Republic of China Ministry of health, and were approved by the local ethics committee. All rabbits were killed by air embolisation six weeks after the OA modeling operation. NZW rabbits were provided by the Fujian University of Traditional Chinese Medicine animal testing center, batch number: SCXK (Shanghai) 2012-0011.

Main reagents and apparatus

Easy nLC Liquid Chromatograph (Thermo Scientific), Q Exactive Mass Spectrometer (Thermo Scientific), AKTA Purifier 100 (GE Healthcare), Multiskan FCMicroplate Photometer (Thermo Scientific), centrifuges (Eppendorf 5430R), Concentrator Plus/Vacufuge (Eppendorf-Concentrator Plus), Electrophoresis (GE Healthcare EPS601), MP Fastprep-24 Automated Homogenizer (MP Biomedicals), ultrasonic liquid processors (ScientzJY92-II, Ningbo), electric thermostatic incubator (Jinghong GNP-9080, Shanghai), vortex (QiTeQT-1, Shanghai), electronic balance (METLER TOLED AL104), MaxQuant 1.3.0.5 (Max Planck Institute of Biochemistry in Martinsried, Germany), Perseus 1.3 (Max Planck Institute of Biochemistry in Martinsried, Germany), glycerol (G0854, Sangon/500 ml), bromophenol blue (161-0404, Sangon), SDS (161-0302, Bio-Rad), urea (161-0731, Bio-Rad), Tris (A6141, Sigma), DTT (161-0404, Bio-Rad), iodoacetamide (IAA, 163-21-09, Bio-Rad), KH_2PO_4 (10017618, Sinopharm), KCl (10016318, Sinopharm), HCl (10011018, Sinopharm), BCA Protein Assay Kit (P0012, Beyotime), Bovine Serum Albumin (BSA) (A0332-25G, Sangon), NH_4HCO_3 (A6141, Sigma), trypsin (317107, Promega), formic acid (FA, 06450, Fluka), trifluoroacetic acid (TFA, T6508, Sigma), acetonitrile (CAN, I592230123, Merck), 10-kDa ultrafiltration tube (Sartorius), C18 cartridge (66872-U, Sigma), Multiple Affinity Removal LC Column-Human 14/Mouse 3 (Agilent), iTRAQ Reagent-4/8 plex Multiplex Kit (AB SCIEX), dissolution buffer (AB SCIEX), SCX chromatography column: Polysulfoethyl 4.6 × 100 mm column (5 μm, 200 Å) (PolyLCInc, Columbia, MD, USA), C18 Trap Column: Thermo Scientific Acclaim PepMap100, 100 μm × 2 cm, nanoViper C18, 3 μm, 100 Å, C18 Analytical Column: Thermo Scientific EASY Column, 10 cm, ID 75 μm, 3 μm, C18-A2, 5 × loading buffer: 10% SDS, 0.5% bromophenol blue, 50% glycerol, 500 mM DTT, 250 mM Tris-HCl, pH 6.8, SDT lysis buffer: 4% SDS, 100 mM Tris-HCl, 1 mM DTT, pH 7.6, UA buffer: 8 M urea, 150 mM Tris-HCl, pH 8.0, SCX Buffer A: 10 mM KH_2PO_4 pH 3.0, 25% CAN, SCX buffer B: 10 mM KH_2PO_4 pH 3.0, 500 mM KCl, 25% CAN, HPLC Buffer A: 0.1% FA, HPLC buffer B: 0.1% FA, 84% CAN.

Animal grouping

Animals were randomly divided into group A (KOA model) or group B (sham KOA model). Each group included eight rabbits.

KOA model

Animals were subjected to right knee anterior cruciate ligament transection (ACLT) as previously described [8]. Rabbits were anesthetized by intraperitoneal injection of 5% chloral hydrate (3 ml/kg). The rabbit was then fixed in the animal-fixing frame, and the right knee shaved and sterilized. A section of the medial joint was revealed. We dislocated the patella and separated and cut the anterior cruciate ligament in group A (ACLT). ACLT was confirmed by Lachman testing by the surgeon. We only dislocated the patella but did not cut the anterior cruciate ligament in group B. After washing the joint with sterile saline, the incision was sealed and sterilized. After the operation the rabbits were housed in separate cages, allowed to move freely, and were routinely cared for.

Specimen collection

Six weeks after ACLT, the rabbits were anesthetized with 5% chloral hydrate. SF samples (0.5 ml) were taken from the knee joint cavity of the suprapatellar bursa, collected in an Eppendorf tube, and condensated for 5 minutes at room temperature. The solution was centrifuged at 12,000 × g for 5 min at room temperature and the supernatant was transferred to a new tube and stored at -80°C for future use.

Protein cleavage and quantification for a label-free experiment

SDT buffer was added to the sample. The lysate was sonicated and then boiled for 15 min. After centrifugation at 14000 g for 40 min, the supernatant was quantified with a BCA Protein

Table 1. The parameters analyzed using Maxquant software

Item	Value
Enzyme	Trypsin
Max Missed Cleavages	2
Max Missed Cleavages	2
Main search	6 ppm
First search	20 ppm
MS/MS Tolerance	20 ppm
Fixed modifications	Carbamidomethyl (C)
Variable modifications	Oxidation (M), Acetyl (Protein N-term)
Database	See the project report
Database pattern	Reverse
Peptide FDR	≤ 0.01
Protein FDR	≤ 0.01
Time window (match between runs)	2 min
Protein Quantification	Razor and unique peptides were used for protein quantification
LFQ [8]	True
LFQ min. ratio count	1

Assay Kit (Bio-Rad, USA). The sample was stored at -80°C.

SDS-PAGE separation

Twenty micrograms of protein from each sample was mixed with 5 × loading buffer and boiled for 5 min, centrifuged at 14000 × g for 10 min and separated by 12.5% SDS-PAGE (14 mA, 90 min). The protein bands were observed by Coomassie Blue R-250 staining.

Filter-aided sample preparation (FASP digestion)

Two hundred micrograms of proteins for each sample were incorporated into 30 μl of SDT buffer (4% SDS, 100 mM DTT, 150 mM Tris-HCl pH 8.0). The detergent, DTT, and other low-molecular-weight components were removed using UA buffer (8 M urea, 150 mM Tris-HCl, pH 8.0) by repeated ultrafiltration (Microcon units, 10 kDa). Then, 100 μl of iodoacetamide (100 mM IAA in UA buffer) was added to block reduced cysteine residues and the samples were incubated for 30 min in the dark. The filters were washed with 100 μl of UA buffer three times and then 100 μl of 25 mM NH_4HCO_3 buffer twice. Finally, the protein suspensions were digested with 4 μg of trypsin (Promega) in 40 μl of 25 mM NH_4HCO_3 buffer overnight at 37°C and the resulting peptides were collected as a filtrate. The peptides of each sample were desalted on C18 Cartridges [Empore™ SPE Cartridges C18 (standard density), bed I.D. 7 mm, volume 3 ml, Sigma], concentrated by vacuum centrifugation, and reconstituted in 40 μl of 0.1% (v/v) formic acid. The peptide content was estimated by UV light spectral density at 280 nm using an extinction coefficient of 1.1 of 0.1% (g/l) solution, which was calculated based on the rate of tryptophan and tyrosine among vertebrate proteins.

Products of protein glycolysis analyzed by LC-MS/MS

LC-MS/MS analysis was performed on a Q Exactive mass spectrometer (Thermo Scientific) that was coupled to Easy nLC (ProxeonBiosystems, now Thermo Fisher Scientific) for 60 min. The mass spectrometer was operated in positive ion mode. MS data were acquired using a data-dependent top 10 method dynamically choosing the most abundant precursor ions from the survey scan (300-1800 m/z) for HCD fragmentation. Automatic gain control (AGC) target was set to 3e6 and maximum injection time to 10 ms. The dynamic exclusion duration was 40.0 s. Survey scans were acquired at a resolution of 70,000 at m/z 200, resolution for HCD spectra was set to 17,500 at m/z 200, and isolation width was 2 m/z. Normalized collision energy was 30 eV and the underfill ratio, which specifies the minimum percentage of the target value likely to be reached at the maximum fill time, was defined as 0.1%. The instru-

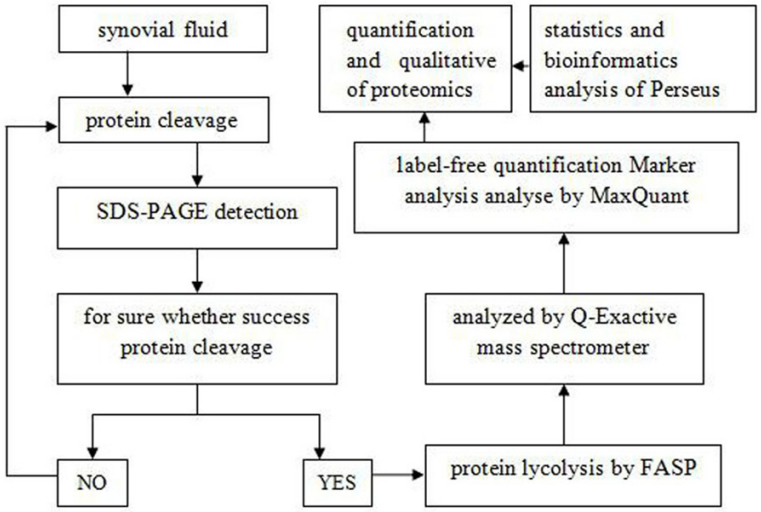

Figure 1. Outline of SF proteome analysis.

Table 2. The protein contents and OD280 levels of peptides in groups A and B

Group	Volume (μl)	Protein contents (μg/μl)	OD280 (μg/μl)
A	200	19.67	1.58
B	200	25.20	1.17

ment was run with peptide recognition mode enabled.

Data analysis by Maxquant software

We analyzed the data using MaxQuant software version 1.3.0.5 (Max Planck Institute of Biochemistry, Martinsried, Germany) [9] The ProteinPilot parameters are presented in **Table 1**.

Statistics and bioinformatic analysis of perseus

The database files from Maxquant were analyzed by Perseus software (version 1.3.0.4). Then Gene Ontology (GO) Annotation, KEGG Pathway Annotation, Hierarchical Clustering and Protein-Protein Interact (PPI) Network analysis were performed. The whole process of SF protein detection is summarized in **Figure 1**.

Quantitated protein sequences were extracted in batch form from the UniProtKB database (2015.03 version) and were stored in FASTA format (201504012FBOYJZXNU.fasta). We used localized sequence software, NCBI BLAST+, to compare the identification of proteins with proteins sequences in the SwissProt Mammalian Database. According to the similarity principle, the functional messages of homologous proteins could be used to note the target proteins. We only reserved the top ten proteins sequences with e-values ≤ 1e-3 for the following analysis.

We then applied the mapping function in Blast2GO (Version 2.8.0) to extract the quantitated proteins sequences which correlated with GO functional items to annotate protein functions.

Proteins do not independently execute their function but act in coordination with other proteins to accomplish biochemical reactions. Thus, the biological processes in cells can be systematically and wholly understood by pathway analysis. KEGG is one of the databases used to study biochemical reaction pathways. We utilized the KEGG Automatic Annotation Server to compare target protein sequences with the KEGG gene database of rabbit protein sequences and then annotated the KO numbers of homologous/similar proteins to the relevant KEGG pathways.

Results

The protein contents of samples and OD280 contents of peptides in the two groups

The protein contents of samples in the two groups are shown in **Table 2**. Group A was 19.67 (μg/μl), group B was 25.20 (μg/μl).

SDS-PAGE analysis

According to the Coomassie brilliant blue atlas, the clear separation of bands of proteins in different groups (**Figure 2**) indicates well extracted protein.

Protein glycolysis analysis by LC-MS/MS in groups A and B

According to the NCBI BLAST and the SwissProt Mammalian database, and with the requirement of a ratio > ±2.0 and $P < 0.05$, we identi-

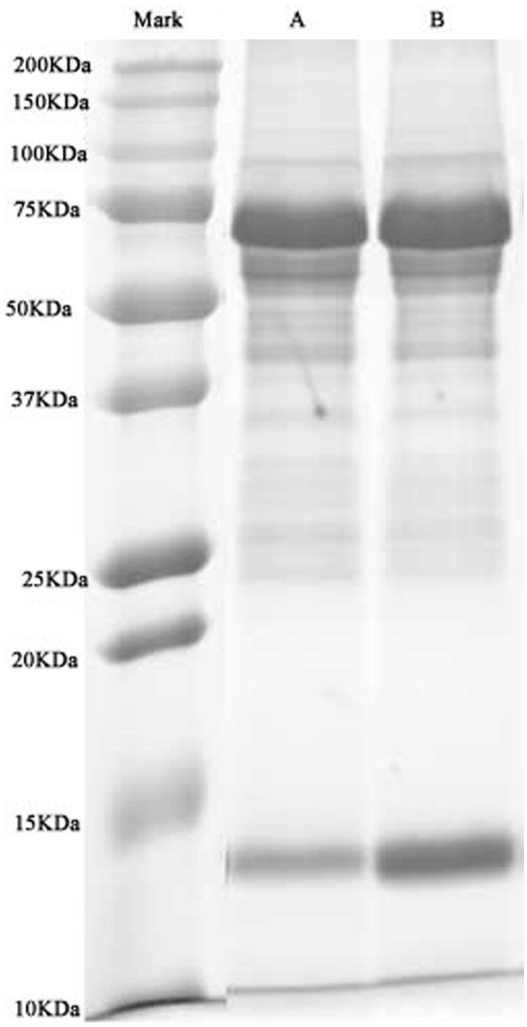

Figure 2. SDS-PAG electrophoregram.

fied 228 proteins in the two groups. We confirmed 23 significantly differentially expressed proteins. The comparable similarity range were 48%-100%, most similarity was ≥ 81% (**Figure 3**).

We extracted 944 relevant items in GO Blast-GO2 for the 239 differentially expressed proteins. We annotated 22 proteins and 450 GO function items, the average level of GO was 7.12 (**Figure 4**).

The final annotation resulted in 23 proteins sequences annotated by 462 GO items. The GO level 2 protein function distribution is shown in the **Figure 5**.

According to the KEGG Automatic Annotation Server, we compared the target protein sequences with rabbit protein sequences in the KEGG gene database, and then annotated the KO numbers of homologous/similar proteins to the relevant KEGG pathways. Finally, we extracted 16 significantly differentially expressed protein sequences including relevant KEGG messages/metabolism pathways (**Table 3**). All of the figures of the annotation pathways were saved in map files, with the significantly differentially expressed proteins highlighted in green. The 16 proteins included adiponectin (ADI), pyruvate kinase (PK/pyk), bisphosphoglycerate mutase (BPGM), heat stroke protein 90A (HSP-90A), hemoglobin subunit α (Hb), viral citrullinated peptide (VCP), 14-3-3 protein β/δ, and ferritin heavy chain (FHC), whose levels were lower in the model group. The other proteins were fibrinogen (Fb) α/β/γ chain, carboxylesterase (CES) 2, paraoxonase/arylesterase 1 (PON-1), apolipoprotein A-I (AopA-1), immunoglobulin heavy chain (IGH), and transferrin (TF), whose levels were lower in the normal group. The results of protein content ratios and significantly differentially expressed proteins in group A and group B are shown in **Table 3**.

Discussion

OA is usually diagnosed according to the combination of symptoms (such as local pain and swelling), and the X-ray or MRI findings (hyperosteogeny or synovial hyperplasia proximal to cartilage lesions, particularly in the bursa suprapatellaris and posterior cruciate ligament of the knee) [2]. The most common pathological change of OA is the progressive degeneration of articular cartilage, but a previous study proposed that synovitis is a significant cause of pain and edema in OA patients [10]. The SF volume can increase because the synovial membrane secretes the SF and its components, such as tumor necrosis factor (TNF) and interleukin (IL), which may undergo biochemical and chemical changes due to the inflammation. Thus, we focused on the synovitis and SF changes in OA.

Although studies have indicated that IL-6, cluster of differentiation 4 (CD4), $CD8^+$ T cells, and adipocytokines (such as adiponectin and leptin) are vital inflammatory factors for the process of synovitis [11, 12], these biomarkers do not have specificity for the diagnosis of synovitis in OA. Over the last 10 years, proteomics has been used to identify and quantify all of the proteins in tissues or cells directly, which

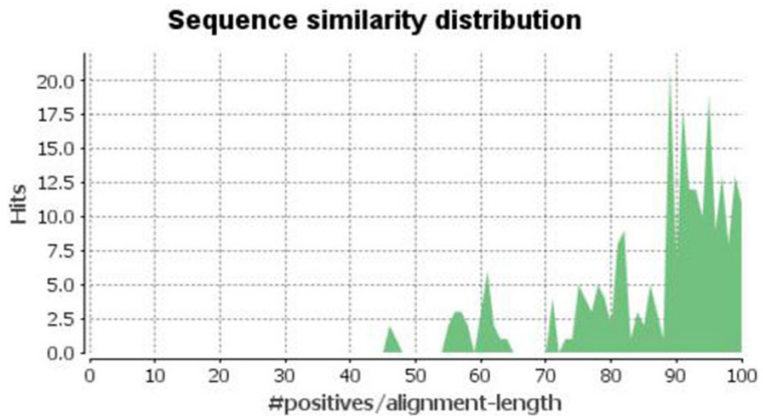

Figure 3. The distribution of sequences comparing similarity.

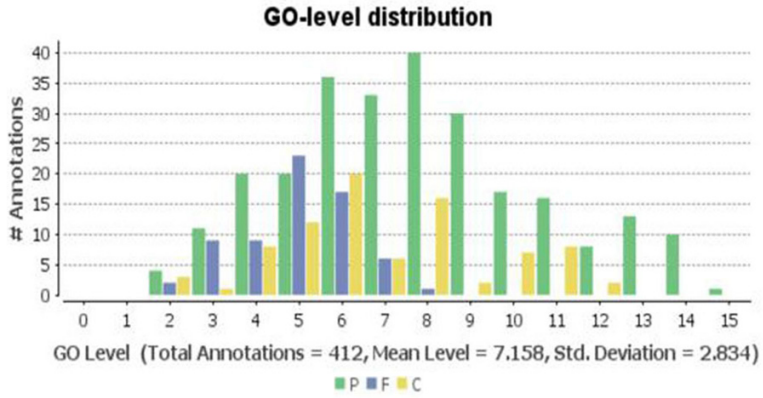

Figure 4. The distribution of GO levels.

has been considered to be a valuable method for elucidating the molecular basis of disease etiology. Recently, the proteomes of human articular chondrocytes, synovial membrane, SF serum, and urine were characterized by two-dimensional polyacrylamide gel electrophoresis (2-DE) and tandem mass spectrometry [5-7, 13-15]. However, to the best of our knowledge, although different proteomic methods have been developed, only the label-free method can authenticate any type of protein, and the advantages of label-free quantitation include that it is rapid and cheap, and does not use a stable isotope as the internal standard [16]. In the present study, we detected the difference of proteomics in SF of KOA model and sham KOA model groups by the label-free method. Our results indicated that the levels of some proteins in SF differed significantly between the KOA model and sham KOA model groups. The different proteins vary in their distributions and functions, which can affect the process of KOA.

By comparison of the differential protein expression patterns in the SF between KOA and sham KOA, we identified 23 functional proteins including 16 proteins that participate in 64 metabolic and transduction pathways. The results demonstrate that the levels of ADI, PK/pyk, BPGM, HSP90A, Hb subunit α, VCP, 14-3-3 protein β/δ/zeta, and FHC proteins were lower in the model group than in the sham model group and that the levels of Fb α/β/γ chain, CES-2, PON-1, AopA-1, IGH, and TF proteins were higher in the model group than in the sham model group. Moreover, the results showed that some proteins, namely, BPGM, Hb subunitα-1 2, VCP/CDC4, 14-3-3 protein β/δ/zeta, FHC, and CES 2, were not identified in the KOA model.

Adiponectin (ADI) is one of the endogenous bioactive peptide compounds involved in the process of OA. The level of ADI was previously reported to be higher in OA patients than in healthy subjects [17]. Other researchers reported that they can detect the expression of the ADI receptor in SF in OA patients [18, 19]. In addition, Francin et al. also reported that ADI was not detected in healthy cartilage, while this adipokine was upregulated in damaged cartilage tissue in OA patients. They found a positive correlation between ADI and MMP-13, while AdipoR1 was related to the expression of type 2 collagen, aggrecan, and Sox9 [20]. Nihan et al. [21] showed that plasma ADI concentrations were associated with both clinical and radiological disease severity in knee OA patients. Moreover, Antonella et al. [22] found that, after mud-bath therapy in patients with knee OA, the ADI, resistin, and visfatin levels in serum decreased significantly. We found that the protein expression in SF was lower in the KOA model group than in the sham model group. Moreover, Chen et al. [23] documented that ADI possesses protective function against OA by regulating the IL-1β-induced expression

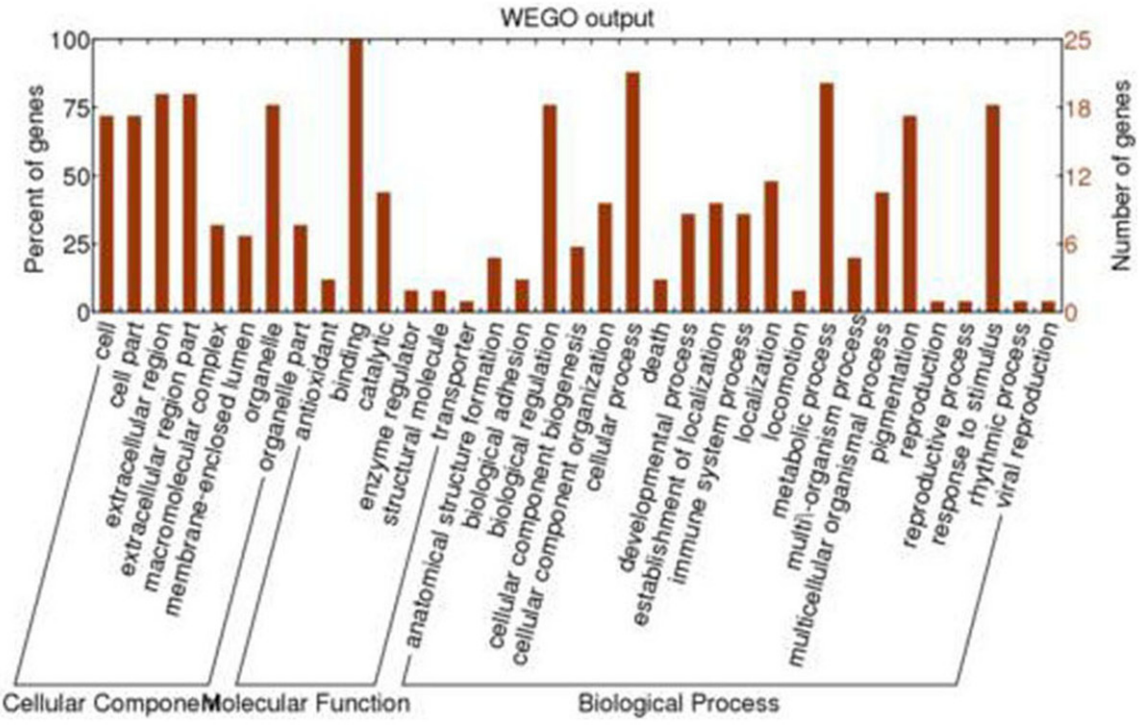

Figure 5. The GO level 2 protein function distribution.

of MMP-13. We speculate that the conflicting findings over the effect of adiponectin on OA may be due to its variable intra-articular content.

There are four PK isoenzymes, LPK, RPK, M1PK, and M2PK [24]. Recently, Bluemlein et al. revealed that M2PK is always the most abundant isoform; it catalyzes the conversion of phosphoenolpyruvate to pyruvate in the pathway of glycolysis [25]. Another study demonstrated that M2PK regulates cell proliferation [26]. Oremek found that the PK concentrations of plasma were increased in patients with rheumatic diseases [27], but the relationship between PK/PYK and OA was not reported. Our results showed that the content of PYK protein was decreased in KOA SF, which can stimulate synovial damage. PKY influences tissue metabolism via the glycolysis, purine metabolism, carbon metabolism, biosynthesis of amino acids, and diabetes mellitus pathways. Our results indicated that PYK may inhibit the process of OA by regulating glycolysis, but this requires further analysis.

BPGM is a multifunctional enzyme that catalyzes both the synthesis and the degradation of 2,3-diphosphoglycerate (2,3-DPG) and exerts three different activities, in that it functions as a 2,3-DPG synthetase, a phosphoglycerate mutase, and a 2,3-DPG phosphatase. In humans, BPGM occurs only in erythrocytes and plays a pivotal role in the dissociation of oxygen from hemoglobin via 2,3-DPG. A further study reported that BPGM activity was decreased in erythrocytes of diabetic patients [28]. However, the relationship of BPGM with OA has not been reported. Wang clarified that BPGM can affect the entire process of histidine phosphorylation [29]. Our results indicated that the content of BPGM protein decreased in SF of the KOA model, which causes synovial damage. According to the KEEG pathway, BPGM takes part in glycolysis, gluconeogenesis, and glycine/serine/threonine metabolism. It may influence the OA process by intervening in erythrocyte metabolism, causing a lack of oxygen, and then inducing the synthesis of cartilage matrix.

Apaf-1 and TNF are closely related to OA, while HSP90 blocks the apoptosis of cells through depressing the oligomerization of Apaf-1 [30, 31]. HSP90 can also inhibit apoptosis induced by TNF through maintaining protein stability during receptor interaction, enhancing NF-kB activities, and regulating the AKT enzyme [32]. Therefore, the HSPs serve as a kind of stress

Table 3. The protein content ratios of the KOA model and normal groups for significantly differentially expressed proteins

Protien ID	KO	Map ID	Pathway	Definition name	*P*-Value	Model/ normal ratio
G1TV17	K07296	ko04152	AMPK	Adiponectin	0.0007531	0.108176237
		ko04920	Adipocytokine			
		ko04932	Non-alcoholic fatty liver disease			
		ko03320	PPAR			
		ko04930	Type II diabetes mellitus			
P11974	K00873	ko00010	Glycolysis/Gluconeogenesis	Pyruvate kinase	0.006569	0.111
		ko00230	Purine metabolism			
		ko00620	Pyruvate metabolism			
		ko01200	Carbon metabolism			
		ko01230	Biosynthesis of amino acids			
		ko04922	Glucagon			
		ko04930	Type II diabetes mellitus			
		ko05203	Viral carcinogenesis			
		ko05230	Central carbon metabolism in cancer			
P07952	K01837	ko00010	Glycolysis/Gluconeogenesis	Bisphosphoglycerate mutase	0.002857	0.129
		ko00260	Glycine, serine and threonine metabolism			
P30946	K04079	ko04141	Protein processing in endoplasmic reticulum	HtpG, HSP90A	0.00010752	0.341
		ko04151	PI3K-Akt signaling pathway			
		ko04612	Antigen processing and presentation			
		ko04621	NOD-like receptor			
		ko04626	Plant-pathogen interaction			
		ko04914	Progesterone-mediated oocyte maturation			
		ko04915	Estrogen signaling pathway			
		ko05200	Pathways in cancer			
		ko05215	Prostate cancer			
G8ZF33	K13822	ko05144	Malaria	Hemoglobin subunit alpha-1 2	0.003087	0.13
G1SR03	K13525	ko04141	Protein processing in endoplasmic reticulum	VCP, CDC4	0.011217	0.139
		ko05134	Legionellosis			
G1T7R2	K06630	ko04110	Cell cycle	14-3-3 protein beta/theta/zeta	0.003154	0.136
		ko04114	Oocyte meiosis			
		ko04391	Hippo			
		ko04722	Neurotrophin signaling pathway			
		ko04151	PI3K-Akt Hippo			
		ko05203	Viral carcinogenesis			
		ko05169	Epstein-Barr virus infection			
G1T6Q8	K03904	ko04978	Mineral absorption	Ferritin heavy chain	0.001823	0.149
G1T0X2	K03903	ko04610	Complement and coagulation cascades	Fibrinogen alpha chain	1.61E-05	4.409
		ko04611	Platelet activation			
G1TZV1	K03927	ko00983	Drug metabolism - other enzymes	Carboxylesterase 2	0.002528	4.501
G1TKX3	K03905	ko04610	Complement and coagulation cascades	Fibrinogen gamma chain	0.000638	4.847
		ko04611	Platelet activation			
		ko05150	Staphylococcus aureus infection			
G1T0W8	K03904	ko04610	Complement and coagulation cascades	Fibrinogen beta chain	0.000568	5.372
		ko04611	Platelet activation			
G1SN96	K01045	ko00363	Bisphenol degradation	Paraoxonase/arylesterase 1	4.66E-06	5.388
		ko00627	Aminobenzoate degradation			
B7NZM1	K08757	ko05143	African trypanosomiasis	Apolipoprotein A-I	9.31E-05	5.883
		ko03320	PPAR			
		ko04975	Fat digestion and absorption			
		ko04977	Vitamin digestion and absorption			

P01879	K06856	ko04020	Calcium signaling	Immunoglobulin heavy chain	0.00053	7.419
		ko04064	NF-kappa B			
		ko04145	Phagosome			
		ko04151	PI3K-Akt			
		ko04640	Hematopoietic cell lineage			
		ko04650	Natural killer cell mediated cytotoxicity			
		ko04662	B cell receptor			
		ko04664	Fc epsilon RI			
		ko04666	Fcgamma R-mediated phagocytosis			
		ko04672	Intestinal immune network for IgA production			
		ko05140	Leishmaniasis			
		ko05143	African trypanosomiasis			
		ko05146	Amoebiasis			
		ko05150	Staphylococcus aureus infection			
		ko05152	Tuberculosis			
		ko05162	Measles			
		ko05169	Epstein-Barr virus infection			
		ko05202	Transcriptional misregulation in cancer			
		ko05310	Asthma			
		ko05320	Autoimmune thyroid disease			
		ko05322	Systemic lupus erythematosus			
		ko05323	Rheumatoid arthritis			
		ko05330	Allograft rejection			
		ko05340	Primary immunodeficiency			
		ko05414	Dilated cardiomyopathy			
		ko05416	Viral myocarditis			
G1TKE4	K14736	ko04978	Mineral absorption	Transferrin	1.32E-05	40.15
		ko04066	HIF-1			

protein, and can affect the differentiation, maturation, and metabolism of chondrocytes. The expression of HSP70 and aggrecan was greatest in the rat OA model group subjected to both microwaves and glutamine administration, in which OA progression was suppressed [33]. Meanwhile, the relationship of HSPs to the SF or synovium has not been reported. Our results indicate that HSPs/90 was lower in SF of the KOA model group, which may be associated with resistance to synovial and cartilage destruction. HSPs/90 influences tissue metabolism by facilitating the processing of proteins in the endoplasmic reticulum, the PI3K-Akt signaling pathway, antigen processing and presentation, the NOD-like receptor signaling pathway, plant-pathogen interaction, progesterone-mediated oocyte maturation, and the estrogen signaling pathway.

Hb of normal human adults is a heterotetramer, $\alpha_2\beta_2$. Because each α subunit has one cysteine residue at αCys104 and each β subunit has two cysteine residues at βCys93 and βCys112, there are three types of (and a total of six) cysteine residues in each hemoglobin molecule. Cysteine residues play a unique role in human Hb by affecting its cooperative oxygen binding behavior and the stability of its tetrameric structure [34]. The correlation of Hb subunit α-1/2 and OA has not been documented. Our results indicate that the level of Hb subunit α-1 2 in the KOA group decreased; Hb subunit α-1 2 may thus convey oxygen to the benefit of cartilage, thereby preventing synovial and cartilage destruction. Huang reported that the β subunit of hemoglobin affects the intramolecular transfer of nitric oxide. We believe that this would impact on the antioxidative effects; specifically, if the level of the β subunit of hemoglobin protein decreased, the process of OA would accelerate [35]. Strader et al. also documented that a novel subunit-specific mechanism in hemoglobin could influence the function of aspartate, the conversion of which increased in β/γ chains with increasing peroxide [36].

Sudha et al. [37] found that VCP antibody in serum was significantly increased in patients with early rheumatoid arthritis; this reveals the viral etiology in early rheumatoid arthritis, and Lucas et al. [38] revealed that VCP protein in-

creased in patients with Paget's disease. Miranda-Hernández et al. found that rituximab for the treatment of RA inhibits B-lymphocyte proliferation through complement-dependent cytotoxicity (CDC) [39]. However, we did not characterize the relationship between VCP and OA. Although no reports on the relationship between CDC with OA have been published, our results revealed that the level of VCP in SF was lower in the KOA group. VCP/CDC4 takes part in the processing of proteins in the endoplasmic reticulum. However, Bateman et al. found that, in OA, genes encoding components of the cell death pathway in mice with osteoarthritis were dysregulated, and endoplasmic reticulum stress transcriptional networks were activated, resulting in further gene dysregulation and the molecular basis of cartilage destruction [40]. Therefore, we think that VCP/CDC4 may prevent synovial and cartilage destruction via the endoplasmic reticulum pathway, but the downregulation of VCP in SF of KOA was contradicted by Bateman's results, so we should obtain further insight into the correlation of VCP and KOA.

14-3-3 proteins are a conserved family of seven isoforms with diverse cellular functions; they are predominantly found intracellularly. The 14-3-3ε isoform is highly expressed in the joints of patients with rheumatoid arthritis and strongly correlates with the expression of metalloproteinases [41]. Sabrina et al. [42] reported that 14-3-3ε is a novel soluble mediator critical in the communication between subchondral bone and cartilage in OA. They speculated that s14-3-3ε is a potential target for a future OA drug. We found that the 14-3-3 protein β/δ/ζ levels were decreased in SF of the KOA model; the 14-3-3 proteins β/δ regulated cell cycle, oocyte meiosis, pathway signaling pathway, neurotrophin signaling pathway, PI3K-Akt signaling pathway, and viral carcinogenesis, the difference between our present results and those of Bateman et al. [40] may be due to some different pathological changes between RA and OA.

HFC is a cellular iron storage protein; it is related to the total body iron status, and affects the oxidative stress reaction in domestic and farm animals. Mewar et al. reported [43] that antiferritin antibodies are observed in a subset of patients with RA, which present early in the disease course and are associated with the severity of radiographic damage. We found that the HFC protein level was decreased in SF in the KOA model; HFC takes part in the protein processing mineral absorption signaling pathway. We know that mineral absorption is very important for bone metabolism and oxidative stress reaction, which is one of the major factors affecting the OA process. In view of this, the relationship between OA and HFC may be an issue for future analysis.

Kong identified three proteins (apolipoprotein, haptoglobin precursor, and fibrinogen D fragment) that are related to joint diseases in SF samples of OA, by using 1DE and 2DE technology [44]. Belcaro et al. found that fibrinogen levels were lowered to 62.8% of initial values after intervention with pycnogenol, which exerts anti-inflammatory activity in osteoarthritic joints [45]. Richette et al. reported that the fibrinogen level was decreased after massive weight loss in obese patients with KOA [46]. Fibrinogen γ and β chains were upregulated in osteoarthritic human synovial tissue [47]. Our results indicate that the Fb protein level in SF of the KOA model was increased compared with that in the sham KOA, which would relieve the inflammation of synovial membrane. Fb affects tissue metabolism by complement and coagulation cascades, and platelet activation pathways.

Satoh et al. [48] divided the CES gene family into CES1, CES2, CES3, CES4, and CES5. The CES2 family includes CES2A1 and CES2A10, which can protect organisms against the entrance of exogenous compounds. However, some researchers have discovered high activity of CESs in the blood of many mammals, including humans [49]. The relationship between carboxylesterase 2 and OA has not previously been documented, but since CES2 plays a leading role in drug metabolism, we consider that it could be a target for treating OA.

PON1 functions in paraoxon hydrolysis. Some studies have indicated that PON1 expression was decreased after the injection of substances such as oxidic LDL, oxidic lipidosome, IL-1β, and TNF-α into HepG2 cells [50]. PON1 activity declined in an environment of oxidative stress, which can cause telomere instability and a decrease in the synthesis of functional glycosaminoglycan in chondrocytes [51]. We assert that the PON family can repress the development of OA because the pathology of this dis-

ease is correlated with both inflammatory factors and stress. This is supported by the reported finding that serum PON1 activity may be a useful adjunctive indicator of the severity of knee OA during follow-up [52]. All of the abovementioned articles focused on the relationship between serum PON and OA, but the expression of PON in SF of OA has rarely been reported. Our results indicated that the PON protein level was upregulated in SF of the KOA model, so we speculate that the inflammatory reaction increases in KOA with the upregulation of PON in SF. PON affects metabolism via the bisphenol degradation and aminobenzoate degradation pathways, but the relationships of these pathways with OA have not been investigated.

Many studies have shown that TNF-α plays a very important role in the pathology of OA. Aspasia et al. found that increasing AopA-1 and AopB levels can enhance the risk of knee OA [53]. Moreover, Okabe et al. showed that APOL-1 mRNA expression decreased in patients with no sign of arthritis [54]. ApoA-1 is a vital factor in the pathogenesis of OA. Our research found that AopA-1 protein expression was higher in SF in the KOA model than in the sham group. We assume that AopA-1 induces synovial and cartilage lesions, and is significantly reduced in normal SF. Moreover, some researchers showed that AopA-1 is the most prominent protein showing a significant decrease in osteopenic femurs [55]. AopA-1 can affect fat digestion and absorption, vitamin digestion and absorption, and influence the course of OA [56, 57].

Immunoglobulin heavy variable chain (IgVH) is involved in the activity of immunoglobulins within the IgA, IgM, and IgG classes [58]. Skriner et al. [59] analyzed the synovial exosomes in patients with RA using electron microscopy, and detected IgG and IgM molecules. Their results demonstrated increases in the levels of fibrin chain fragment, fibrinogen chain precursor, and fibrinogen D fragment, which are related to the metabolism of antibodies. Studies have also shown that Ig variable H chain (VH) gene usage by synovial B cells in OA yielded conflicting results with regard to clonal expansion and somatic hypermutation [60-62]. Our study showed that the IgVH protein expression in SF is higher in the KOA model group than in the sham group. We thus assume that the functions of IgVH may further aggravate synovial inflammation and cartilage damage. Reng-Rong [63] et al. discovered that the synovial membrane in OA patients contains the Ig H chain variable region (VH) genes of B cells.

TF/TRF transfers Fe into cells, the correlation between TF and osteoarticular diseases has been studied. Alexander et al. [64] suggested that the role of transferrin is not vital for chondrocyte survival or matrix synthesis. Chales et al. regarded arthropathy as a major and distinctive manifestation of hemochromatosis, resembling degenerative joint disease with involvement of unusual articular sites, almost identical to the arthropathy in calcium pyrophosphate dihydrate crystals deposition disease (chondrocalcinosis); early biomarkers show increasing serum tranferrin saturation [65]. Huleihel et al. found that IL-1 can induce TRF secretion from Sertoli cells *in vitro*, meaning that a reduced IL1 content would inhibit the TRF level [66]. In the present study, we found that TF protein content was higher in SF of the KOA model group than in the sham KOA model group, indicating that TRF enhances inflammation and affects the progression of KOA through mineral absorption and the HIF-1 signaling pathway [67].

In conclusion, our results demonstrated that the levels of ADI, PK/pyk, BPGM, HSP90A, Hb subunit α, VCP, 14-3-3 protein β/δ, and FHC proteins were decreased and those of the Fb α/β/γ chain, CES-2, PON-1, AopA-1, IGH, and TF proteins were increased in SF of the KOA model. In addition, we found that the ratio of ADI and TF was lowest in the KOA model group and highest in the sham KOA model group, so regulating the content of ADI and TF may provide a new approach for treating KOA.

Acknowledgements

This work was supported by the National Natural Science Foundation of China (No. 8127-3774).

Disclosure of conflict of interest

None.

Address correspondence to: Ning Yang, The Fifth Affiliated Hospital of Guangzhou Medicine University, No. 621, Gangwan Road, Huangpu District of Guangzhou Municipality, Guangzhou 510700, Gu-

angdong, China. Tel: +8620-82285847; Fax: +8620-82285847; E-mail: 1443572213@qq.com

References

[1] Krasnokutsky S, Attur M, Palmer G, Samuels J, Abramson SB. Current concepts in the pathogenesis of osteoarthritis. Osteoarthritis Cartilage 2008; 16: S1-3.

[2] Hayashi D, Roemer FW, Katur A, Felson DT, Yang SO, Alomran F, Guermazi A. Imaging of synovitis in osteoarthritis: current status and outlook. Semin Arthritis Rheum 2011; 41: 116-130.

[3] Scanzello CR, Goldring SR. The role of synovitis in osteoarthritis pathogenesis. Bone 2012; 51: 249-257.

[4] Guo H, Luo Q, Zhang J, Lin H, Xia L, He C. Comparing different physical factors on serum TNF-α levels, chondrocyte apoptosis, caspase-3 and caspase-8 expression in osteoarthritis of the knee in rabbits. Joint Bone Spine 2011; 78: 604-610.

[5] Ritter SY, Subbaiah R, Bebek G, Crish J, Scanzello CR, Krastins B, Sarracino D, Lopez MF, Crow MK, Aigner T, Goldring MB, Goldring SR, Lee DM, Gobezie R, Aliprantis AO. Proteomic analysis of synovial fluid from the osteoarthritic knee: comparison with transcriptome analyses of joint tissues. Arthritis Rheum 2013; 65: 981-992.

[6] Balakrishnan L, Bhattacharjee M, Ahmad S, Nirujogi RS, Renuse S, Subbannayya Y, Marimuthu A, Srikanth SM, Raju R, Dhillon M, Kaur N, Jois R, Vasudev V, Ramachandra Y, Sahasrabuddhe NA, Prasad TsK, Mohan S, Gowda H, Shankar S, Pandey A. Differential proteomic analysis of synovial fluid from rheumatoid arthritis and osteoarthritis patients. Clin Proteomics 2014; 11: 1.

[7] Ikeda D, Ageta H, Tsuchida K, Yamada H. iTRAQ-based proteomics reveals novel biomarkers of osteoarthritis. Biomarkers 2013; 18: 565-572.

[8] Batiste DL, Kirkley A, Laverty S, Thain LM, Spouge AR, Gati JS, Foster PJ, Holdsworth DW. High-resolution MRI and micro-CT in an ex vivo rabbit anterior cruciate ligament transection model of osteoarthritis. Osteoarthritis Cartilage 2004; 12: 614-626.

[9] Cox J, Mann M. MaxQuant enables high peptide identification rates, individualized p.p.b.-range mass accuracies and proteome-wide protein quantification. Nat Biotechnol 2008; 26: 1367-1372.

[10] de Lange-Brokaar BJ, Ioan-Facsinay A, Yusuf E, Visser AW, Kroon HM, van Osch GJ, Zuurmond AM, Stojanovic-Susulic V, Bloem JL, Nelissen RG, Huizinga TW, Kloppenburg M. Association of pain in knee osteoarthritis with distinct patterns of synovitis. Arthritis Rheumatol 2015; 67: 733-740.

[11] Pawłowska J, Mikosik A, Soroczynska-Cybula M, Jóźwik A, Łuczkiewicz P, Mazurkiewicz S, Lorczyński A, Witkowski JM, Bryl E. Different distribution of CD4 and CD8 T cells in synovial membrane and peripheral blood of rheumatoid arthritis and osteoarthritis patients. Folia Histochem Cytobiol 2009; 47: 627-632.

[12] Presle N, Pottie P, Dumond H, Guillaume C, Lapicque F, Pallu S, Mainard D, Netter P, Terlain B. Differential distribution of adipokines between serum and synovial fluid in patients with osteoarthritis. Contribution of joint tissues to their articular production. Osteoarthritis Cartilage 2006; 14: 690-695.

[13] Fernández-Costa C, Calamia V, Fernández-Puente P, Capelo-Martínez JL, Ruiz-Romero C, Blanco FJ. Sequential depletion of human serum for the search of osteoarthritis biomarkers. Proteome Sci 2012; 10: 55.

[14] Henrotin Y, Gharbi M, Mazzucchelli G, Dubuc JE, De Pauw E, Deberg M. Fibulin 3 peptides Fib3-1 and Fib3-2 are potential biomarkers of osteoarthritis. Arthritis Rheum 2012; 64: 2260-2267.

[15] Mobasheri A. Osteoarthritis year 2012 in review: biomarkers. Osteoarthritis Cartilage 2012; 20: 1451-1464.

[16] Tu L, Li X, Bian S, Yu Y, Li J, Huang L, Liu P, Wu Q, Wang W. Label-free and real-time monitoring of single cell attachment on template-stripped plasmonic nano-holes. Sci Rep 2017; 7: 11020.

[17] Laurberg TB, Frystyk J, Ellingsen T, Hansen IT, Jørgensen A, Tarp U, Hetland ML, Hørslev-Petersen K, Hornung N, Poulsen JH, Flyvbjerg A, Stengaard-Pedersen K. Plasma adiponectin in patients with active, early, and chronic rheumatoid arthritis who are steroid- and disease-modifying antirheumatic drug-naive compared with patients with osteoarthritis and controls. J Rheumatol 2009; 36: 1885-1891.

[18] Junker S, Frommer KW, Krumbholz G. Expression of adipocytokines in osteoarthritis osteophytes. Osteoarthritis Cartilage 2012; 20: S115-S115.

[19] Hao D, Li M, Wu Z, Duan Y, Li D, Qiu G. Synovial fluid level of adiponectin correlated with levels of aggrecan degradation markers in osteoarthritis. Rheumatol Int 2011; 31: 1433-1437.

[20] Francin PJ, Abot A, Guillaume C, Moulin D, Bianchi A, Gegout-Pottie P, Jouzeau JY, Mainard D, Presle N. Association between adiponectin and cartilage degradation in human osteoarthritis. Osteoarthritis Cartilage 2014; 22: 519-526.

[21] Cuzdan Coskun N, Ay S, Evcik FD, Oztuna D. Adiponectin: is it a biomarker for assessing the disease severity in knee osteoarthritis patients? Int J Rheum Dis 2017; 20: 1942-1949.
[22] Fioravanti A, Giannitti C, Cheleschi S, Simpatico A, Pascarelli NA, Galeazzi M. Circulating levels of adiponectin, resistin, and visfatin after mud-bath therapy in patients with bilateral knee osteoarthritis. Int J Biometeorol 2015; 59: 1691-1700.
[23] Chen TH, Chen L, Hsieh MS, Chang CP, Chou DT, Tsai SH. Evidence for a protective role for adiponectin in osteoarthritis. Biochim Biophys Acta 2006; 1762: 711-718.
[24] Yamada K, Noguchi T. Nutrient and hormonal regulation of pyruvate kinase gene expression. Biochem J 1999; 337: 1-11.
[25] Bluemlein K, Grüning NM, Feichtinger RG, Lehrach H, Kofler B, Ralser M. No evidence for a shift in pyruvate kinase PKM1 to PKM2 expression during tumorigenesis. Oncotarget 2011; 2: 393-400.
[26] Morgan HP, O'Reilly FJ, Wear MA, O'Neill JR, Fothergill-Gilmore LA, Hupp T, Walkinshaw MD. M2 pyruvate kinase provides a mechanism for nutrient sensing and regulation of cell proliferation. Proc Natl Acad Sci U S A 2013; 110: 5881-5886.
[27] Oremek GM, Müller R, Sapoutzis N, Wigand R. Pyruvate kinase type tumor M2 plasma levels in patients afflicted with rheumatic diseases. Anticancer Res 2003; 23: 1131-1134.
[28] Fujita T, Suzuki K, Tada T, Yoshihara Y, Hamaoka R, Uchida K, Matuo Y, Sasaki T, Hanafusa T, Taniguchi N. Human erythrocyte bisphosphoglycerate mutase: inactivation by glycation in vivo and in vitro. J Biochem 1998; 124: 1237-1244.
[29] Wang Y, Liu L, Wei Z, Cheng Z, Lin Y, Gong W. Seeing the process of histidine phosphorylation in human bisphosphoglycerate mutase. J Biol Chem 2006; 281: 39642-8.
[30] Taylor RP, Benjamin IJ. Small heat shock proteins: a new classification scheme in mammals. J Mol Cell Cardiol 2005; 38: 433-444.
[31] Kamradt MC, Lu M, Werner ME, Kwan T, Chen F, Strohecker A, Oshita S, Wilkinson JC, Yu C, Oliver PG, Duckett CS, Buchsbaum DJ, LoBuglio AF, Jordan VC, Cryns VL. The small heat shock protein alpha B-crystallin is a novel inhibitor of TRAIL-induced apoptosis that suppresses the activation of caspase-3. J Biol Chem 2005; 280: 11059-11066.
[32] Lewis J, Devin A, Miller A, Lin Y, Rodriguez Y, Neckers L, Liu ZG. Disruption of hsp90 function results in degradation of the death domain kinase, receptor-interacting protein (RIP), and blockage of tumor necrosis factor-induced nuclear factor-kappaB activation. J Biol Chem 2000; 275: 10519-10526.
[33] Fujita S, Arai Y, Nakagawa S, Takahashi KA, Terauchi R, Inoue A, Tonomura H, Hiraoka N, Inoue H, Tsuchida S, Mazda O, Kubo T. Combined microwave irradiation and intraarticular glutamine administration-induced HSP70 expression therapy prevents cartilage degradation in a rat osteoarthritis model. J Orthop Res 2012; 30: 401-407.
[34] Kan HI, Chen IY, Zulfajri M, Wang CC. Subunit disassembly pathway of human hemoglobin revealing the site-specific role of its cysteine residues. J Phys Chem B 2013; 117: 9831-9839.
[35] Huang KT, Azarov I, Basu S, Huang J, Kim-Shapiro DB. Lack of allosterically controlled intramolecular transfer of nitric oxide from the heme to cysteine in the beta subunit of hemoglobin. Blood 2006; 107: 2602-2604.
[36] Strader MB, Hicks WA, Kassa T, Singleton E, Soman J, Olson JS, Weiss MJ, Mollan TL, Wilson MT, Alayash AI. Post-translational transformation of methionine to aspartate is catalyzed by heme iron and driven by peroxide: a novel subunit-specific mechanism in hemoglobin. J Biol Chem 2014; 289: 22342-22357.
[37] Deo SS, Shetty RR, Mistry KJ, Chogle AR. Detection of viral citrullinated peptide antibodies directed against EBV or VCP: in early rheumatoid arthritis patients of Indian origin. J Lab Physicians 2010; 2: 93-99.
[38] Lucas GJ, Mehta SG, Hocking LJ, Stewart TL, Cundy T, Nicholson GC, Walsh JP, Fraser WD, Watts GD, Ralston SH, Kimonis VE. Evaluation of the role of valosin-containing protein in the pathogenesis of familial and sporadic Paget's disease of bone. Bone 2006; 38: 280-285.
[39] Miranda-Hernández MP, López-Morales CA, Ramírez-Ibáñez ND, Piña-Lara N, Pérez NO, Molina-Pérez A, Revilla-Beltri J, Flores-Ortiz LF, Medina-Rivero E. Assessment of physicochemical properties of rituximab related to its immunomodulatory activity. J Immunol Res 2015; 2015: 910763.
[40] Bateman JF, Rowley L, Belluoccio D, Chan B, Bell K, Fosang AJ, Little CB. Transcriptomics of wild-type mice and mice lacking ADAMTS-5 activity identifies genes involved in osteoarthritis initiation and cartilage destruction. Arthritis Rheum 2013; 65: 1547-1560.
[41] Maksymowych WP, Marotta A. 14-3-3η: a novel biomarker platform for rheumatoid arthritis. Clin Exp Rheumatol 2014; 32: S35-39.
[42] Priam S, Bougault C, Houard X, Gosset M, Salvat C, Berenbaum F, Jacques C. Identification of soluble 14-3-3ε as a novel subchondral bone mediator involved in cartilage degrada-

tion in osteoarthritis. Arthritis Rheum 2013; 65: 1831-1842.
[43] Mewar D, Moore DJ, Young-Min S, Bertolaccini ML, Khamashta MA, Watson PF, Wilson AG. Antiferritin antibodies discovered by phage display expression cloning are associated with radiographic damage in rheumatoid arthritis. Arthritis Rheum 2005; 52: 3868-3872.
[44] Kong MK, Min BH, Lee PC. Evaluation of a pretreatment method for two-dimensional gel electrophoresis of synovial fluid using cartilage oligomeric matrix protein as a marker. J Microbiol Biotechnol 2012; 22: 654-658.
[45] Belcaro G, Cesarone MR, Errichi S, Zulli C, Errichi BM, Vinciguerra G, Ledda A, Di Renzo A, Stuard S, Dugall M, Pellegrini L, Gizzi G, Ippolito E, Ricci A, Cacchio M, Cipollone G, Ruffini I, Fano F, Hosoi M, Rohdewald P. Variations in C-reactive protein, plasma free radicals and fibrinogen values in patients with osteoarthritis treated with pycnogenol. Redox Rep 2008; 13: 271-276.
[46] Richette P, Poitou C, Garnero P, Vicaut E, Bouillot JL, Lacorte JM, Basdevant A, Clément K, Bardin T, Chevalier X. Benefits of massive weight loss on symptoms, systemic inflammation and cartilage turnover in obese patients with knee osteoarthritis. Ann Rheum Dis 2011; 70: 139-144.
[47] Cillero-Pastor B, Eijkel GB, Blanco FJ, Heeren RM. Protein classification and distribution in osteoarthritic human synovial tissue by matrix-assisted laser desorption ionization mass spectrometry imaging. Anal Bioanal Chem 2015; 407: 2213-2222.
[48] Satoh T, Hosokawa M. Structure, function and regulation of carboxylesterases. Chem Biol Interact 2006; 162: 195-211.
[49] Li B, Sedlacek M, Manoharan I, Boopathy R, Duysen EG, Masson P, Lockridge O. Butyrylcholinesterase, paraoxonase, and albumin esterase, but not carboxylesterase, are present in human plasma. Biochem Pharmacol 2005; 70: 1673-1684.
[50] Van Lenten BJ, Wagner AC, Navab M, Fogelman AM. Oxidized phospholipids induce changes in hepatic paraoxonase and ApoJ but not monocyte chemoattractant protein-1 via interleukin-6. J Biol Chem 2001; 276: 1923-1929.
[51] Yudoh K, Nguyen vT, Nakamura H, Hongo-Masuko K, Kato T, Nishioka K. Potential involvement of oxidative stress in cartilage senescence and development of osteoarthritis: oxidative stress induces chondrocyte telomere instability and downregulation of chondrocyte function. Arthritis Res Ther 2005; 7: R380-391.
[52] Ertürk C, Altay MA, Selek S, Koçyiğit A. Paraoxonase-1 activity and oxidative status in patients with knee osteoarthritis and their relationship with radiological and clinical parameters. Scand J Clin Lab Invest 2012; 72: 433-439.
[53] Tsezou A, Iliopoulos D, Malizos KN, Simopoulou T. Impaired expression of genes regulating cholesterol efflux in human osteoarthritic chondrocytes. J Orthop Res 2010; 28: 1033-1039.
[54] Okabe T, Ohmori Y, Tanigami A, Hishigaki H, Suzuki Y, Sugano S, Kawaguchi A, Nakaya H, Wakitani S. Detection of gene expression in synovium of patients with osteoarthritis using a random sequencing method. Acta Orthop 2007; 78: 687-692.
[55] Chaput CD, Dangott LJ, Rahm MD, Hitt KD, Stewart DS, Wayne Sampson H. A proteomic study of protein variation between osteopenic and age-matched control bone tissue. Exp Biol Med (Maywood) 2012; 237: 491-498.
[56] Jingbo W, Aimin C, Qi W, Xin L, Huaining L. Betulinic acid inhibits IL-1β-induced inflammation by activating PPAR-γ in human osteoarthritis chondrocytes. Int Immunopharmacol 2015; 29: 687-692.
[57] Lacki JK, Klama K, Mackiewicz SH. Immunoglobulin A--alpha-1-antitrypsin complex in rheumatic diseases. Mater Med Pol 1996; 28: 138-140.
[58] Skriner K, Adolph K, Jungblut PR, Burmester GR. Association of citrullinated proteins with synovial exosomes. Arthritis Rheum 2006; 54: 3809-3814.
[59] Krenn V, Hensel F, Kim HJ, Souto Carneiro MM, Starostik P, Ristow G, König A, Vollmers HP, Müller-Hermelink HK. Molecular IgV(H) analysis demonstrates highly somatic mutated B cells in synovialitis of osteoarthritis: a degenerative disease is associated with a specific, not locally generated immune response. Lab Invest 1999; 79: 1377-1384.
[60] Magalhães R, Gehrke T, Souto-Carneiro MM, Kriegsmann J, Krenn V. Extensive plasma cell infiltration with crystal IgG inclusions and mutated IgV(H) gene in an osteoarthritis patient with lymphoplasmacellular synovitis. A case report. Pathol Res Pract 2002; 198: 45-50.
[61] Shiokawa S, Matsumoto N, Nishimura J. Clonal analysis of B cells in the osteoarthritis synovium. Ann Rheum Dis 2001; 60: 802-805.
[62] Da RR, Qin Y, Baeten D, Zhang Y. B cell clonal expansion and somatic hypermutation of Ig variable heavy chain genes in the synovial membrane of patients with osteoarthritis. J Immunol 2007; 178: 557-565.
[63] Cigan AD, Nims RJ, Albro MB, Esau JD, Dreyer MP, Vunjak-Novakovic G, Hung CT, Ateshian

GA. Insulin, ascorbate, and glucose have a much greater influence than transferrin and selenous acid on the in vitro growth of engineered cartilage in chondrogenic media. Tissue Eng Part A 2013; 19: 1941-1948.
[64] Chalès G, Guggenbuhl P, Pawlotsky Y. [Iron overload and arthropathy]. Rev Prat 2006; 56: 2135-2140.
[65] Huleihel M, Zeyse D, Lunenfeld E, Zeyse M, Mazor M. Induction of transferrin secretion in murine Sertoli cells by FSH and IL-1: the possibility of different mechanism(s) of regulation. Am J Reprod Immunol 2002; 47: 112-117.
[66] Zhang FJ, Luo W, Lei GH. Role of HIF-1α and HIF-2α in osteoarthritis. Joint Bone Spine 2015; 82: 144-147.
[67] Karaaslan F, Mutlu M, Mermerkaya MU, Karaoğlu S, Saçmaci Ş, Kartal Ş. Comparison of bone tissue trace-element concentrations and mineral density in osteoporotic femoral neck fractures and osteoarthritis. Clin Interv Aging 2014; 9: 1375-1378.